IOPscience iopscience.iop.org

Home Search Collections Journals About Contact us My IOPscience

Evolving properties of two-dimensional materials: from graphene to graphite

This article has been downloaded from IOPscience. Please scroll down to see the full text article.

2009 J. Phys.: Condens. Matter 21 335502

(http://iopscience.iop.org/0953-8984/21/33/335502)

View the table of contents for this issue, or go to the journal homepage for more

Download details:
IP Address: 129.252.86.83
The article was downloaded on 29/05/2010 at 20:44

Please note that terms and conditions apply.

IOP Publishing Journal of Physics: Condensed Matter

J. Phys.: Condens. Matter **21** (2009) 335502 (7pp) doi:10.1088/0953-8984/21/33/335502

Evolving properties of two-dimensional materials: from graphene to graphite

M Klintenberg[1,3], S Lebègue[2], C Ortiz[1], B Sanyal[1], J Fransson[1] and O Eriksson[1]

[1] Department of Physics and Materials Science, Uppsala University, Box 530, 751 21 Uppsala, Sweden

[2] Laboratoire de Cristallographie, Résonance Magnétique et Modélisations (CRM2, UMR CNRS 7036) Institut Jean Barriol, Nancy Université BP 239, Boulevard des Aiguillettes 54506 Vandoeuvre-lès-Nancy, France

E-mail: Mattias.Klintenberg@fysik.uu.se

Received 3 June 2009, in final form 7 July 2009
Published 27 July 2009
Online at stacks.iop.org/JPhysCM/21/335502

Abstract

We have studied theoretically, using density functional theory, several material properties when going from one C layer in graphene to two and three graphene layers and on to graphite. The properties we have focused on are the elastic constants, electronic structure (energy bands and density of states), and the dielectric properties. For any of the properties we have investigated the modification due to an increase in the number of graphene layers is within a few per cent. Our results are in agreement with the analysis presented recently by Kopelevich and Esquinazi (unpublished).

(Some figures in this article are in colour only in the electronic version)

1. Introduction

The recent explosion of scientific activity around the newly discovered two-dimensional material graphene is unprecedented since the discovery of the high temperature superconductors in the late 1980s [1–5]. The uniqueness of this material, and the technological advantages it promises, gathers researchers from different scientific fields. As in many previous major scientific breakthroughs, the main component for the success story of graphene was the actual synthesis of the material [6]. Unexpectedly, Novoselov *et al* were able to fabricate a truly two-dimensional material and free-standing single graphene layers, the building block of graphite, produced by means of exfoliation. Graphene can also be grown on SiC by epitaxial growth. In addition, growth of graphene on catalytic surfaces (e.g. Ni or Pt) has been demonstrated. An insulating thicker material can be grown on top and after chemically removing the primary layer one is left with a single atomic layer of graphene on an insulating substrate [1].

Research on graphene was initially motivated by a highly spectacular phenomenon, namely mass-less Dirac fermions. Although there is nothing relativistic in the single electron Kohn–Sham Hamiltonian describing the electronic structure of graphene, the band dispersion turns out to have a very unique property, at least from calculations based on the local density approximation (LDA) and the generalized gradient approximation (GGA), which enables a comparison to quasiparticle states obtained from the Dirac equation, with an effective speed of light of 10^6 m s^{-1} [1, 3] and zero rest mass.

Studies of the electronic properties of graphene have revealed an ambipolar electric field effect, with high concentrations and high mobility (up to 15.000 cm^2 V^{-1} s^{-1}). In addition, conductivity properties reveal ballistic transport on the submicrometer scale, which is unexpected not least due to the measurements not being performed in ultrahigh vacuum, and hence many different molecular species are expected to be absorbed and act as scattering centers. Furthermore, graphene is the only material know to date with a quantum Hall effect (QHE) at room temperature [7], and the QHE was shown to be somewhat anomalous in nature [7]. The realization of a material with negative index of refraction for electrons has also been demonstrated in graphene, because the electron states in the valence band have a group velocity antiparallel to the k-vector. Hence, the Veselago lens, which has the unique property of having a resolution not determined by

[3] Author to whom any correspondence should be addressed.

 © 2009 IOP Publishing Ltd Printed in the UK

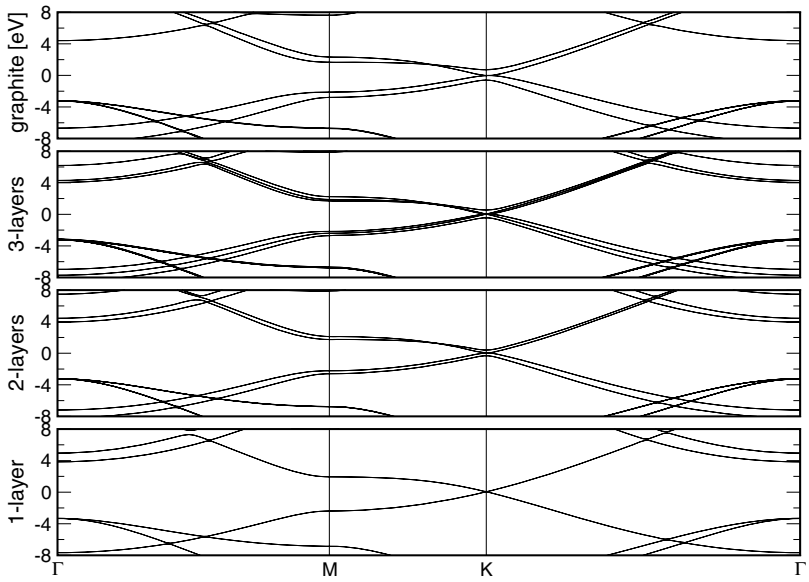

Figure 1. The LDA electronic band structure for one-, two-, and three-layer graphene and graphite. The linear bands around the K-point near the Fermi level can be seen for one- and three-layer graphene, i.e. odd numbers of layers.

the wavelength, has been demonstrated in applications with graphene [8].

The focus of the present paper is to investigate how the electronic properties of graphene evolve to those of graphite, by a systematic theoretical study of one, two and three layers of graphene. We will make comparisons between the calculated results and existing data for graphite, and in this way we will shine some light on how the electronic structure of sp^2 bonded C layers evolves from that of graphene to that of graphite. The properties we focus on here are the electronic structure, the dielectric function, $\epsilon(\omega)$, and the elastic constants.

2. Details of calculations

The electronic structure and elastic constants have been calculated using a highly accurate full potential linear muffin-tin orbital (FP-LMTO) method [9] within the local density approximation (LDA). A $18 \times 18 \times 1$ k-point grid gave converged results ($18 \times 18 \times 6$ for graphite) and for the density of states a $36 \times 36 \times 12$ k-point mesh was used to avoid numerical difficulties with the tetrahedron integration. The FP-LMTO and PAW (see below) results are found to agree nicely. In the FP-LMTO method the wavefunction in the interstitial region is expanded using Bloch sums of spherical Hankel or Neumann functions and in the muffin-tin region the basis is a linear combination of spherical waves. The latter linear muffin-tin orbitals have a high angular momentum character in them due to a large angular momentum truncation in the so-called structure constant. Therefore d-character in the density of states can be seen even though an sp basis set is used. A 2sp3sp basis set was necessary to obtain the correct electronic structure (compare with the minimal 2sp basis set) and the muffin-tin radii were optimized to cover 90% of the nearest neighbor distance.

The calculations of the optical properties have been performed using the VASP (Vienna *Ab initio* Simulation Package) code [10, 11], implementing the PAW formalism [12]. We have used the PBE exchange–correlation functional [13]. To ensure negligible interaction between periodic images, a large value (20 Å) of the cell parameter 'c' was used. The convergence of the dielectric function is obtained by using a $80 \times 80 \times 5$ Monkhorst–Pack mesh [14]. For the plane wave expansion of the wavefunction a 400 eV cut-off was used.

For two-, and three-layer graphene AB and ABA stackings were used, respectively. The interlayer distance used was 3.35 Å. The LDA and GGA functionals do not capture the effects of the van der Waals interaction. However, in this paper we do not focus on the van der Waals bonds between the graphene planes. Instead we focus on the electronic structure, dielectric function, and chemical bonding within the graphene planes, and for these properties LDA and GGA are expected to be accurate.

3. Results

3.1. Electronic structure from a FP-LMTO model

The energy bands for one, two, and three graphene layers are shown in figure 1. For graphite and one- and few-layer graphene we find an electronic structure which is similar to that found by others [15–20]. References [15, 16] are classical papers on graphite band structure. References [17, 18] report Raman results on two-layer graphene, and [19, 20] present tight-binding results for one- and few-layer graphene. In [21] a GW calculation of graphene is presented and it is noted that the one-layer band structure presented here is in close agreement with the LDA band structure of this reference. However, a small difference (0.5 eV) of the band-gap at the Γ-point is noted which could be an effect of different atomic

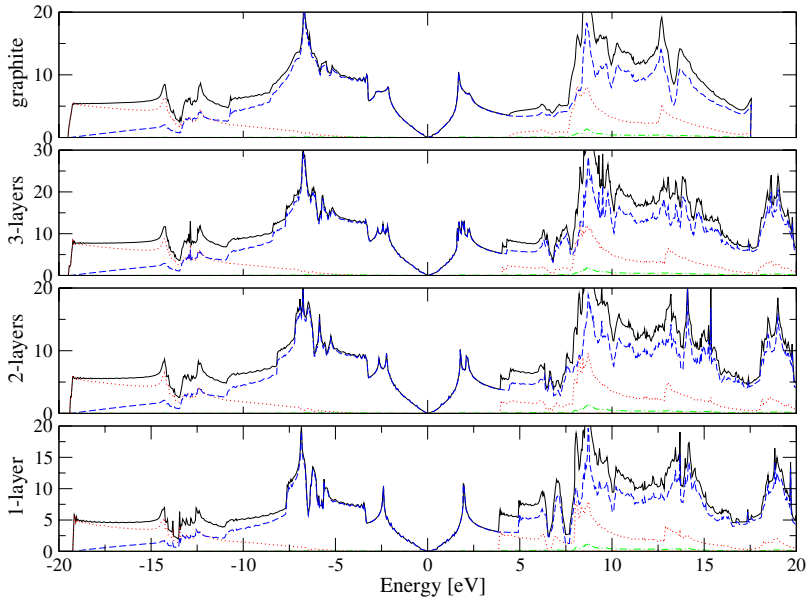

Figure 2. The density of states for one-, two-, and three-layer graphene and graphite. Colored lines show l-resolved partial DOS, s (dot, red), p (dash, blue), and d (dot–dash, green). The black full line shows total DOS.

representation (basis set). For a detailed discussion on carbon basis sets and eigenvalues at Γ in graphite see [22, 23]. At the K-point two energy bands of p_z character cut the Fermi level (E_F), and the energy dispersion is (close to) linear with respect to the crystal momentum. This represents the bands referred to as mass-less Dirac fermion states. For two layers the number of energy bands doubles, and there are four sets of p_z derived bands close to the K-point. Due to the interaction between the graphene layers, these bands split apart so that only two bands cut E_F, and the energy dispersion deviates more from linear compared to the situation for one layer. For three layers a set of six p_z derived bands can be found close to E_F at the K-point. In this case four bands cut E_F and two bands split apart. The electronic band structure for three layers looks like a combination of the band structures for one- and two-layer graphene, including two linear bands close to the K-point. In general figure 1 suggests that the more carbon layers that are introduced, the wider energy range does the set of p_z bands span. This saturates for bulk graphite where in addition to the degenerate bands at E_F there is one band ∼0.7 eV above E_F and one band ∼0.7 eV below E_F [22].

The corresponding densities of states (DOSs) are shown in figure 2. Around the Fermi level the electrons (holes) have p-character. The overall structure of the PDOS is similar for all four cases. The main differences occur at the first van Hove singularity at ±2 eV where graphene has a clear singularity and few-layer graphenes have a more complex structure. A complex structure is also seen at −5 to −7 eV but in this case the complexity is decreasing with the number of layers. The latter decrease in complexity is also seen at around 4 eV where for one-layer graphene there is a clear step-like pattern. These steps occur when the 3s component increases. We note that the inclusion of a 3sp basis is crucial for correct electronic structure results.

Some experiments, using either the de Haas–van Alphen effect [25], or the quantum Hall effect [26], have shown that electrons and holes with linear dispersion relations could exist not only in graphene but also in graphite. Dirac fermions were also predicted in silicene [27] from *ab initio* calculations. In fact, it was shown using a tight-binding description of the electronic structure [28] that Dirac fermions exist in graphene multilayers if the number of layers is odd (systems with a mirror inversion plane). However, tight-binding calculations depend on a given set of parameters, and although they can provide clues about the general mechanisms, they are not as precise as *ab initio* calculations. Therefore it was important to check whether the above assumptions are still valid when obtained from *ab initio* calculations. We computed precisely the electronic structure of each system around the K-point, as shown in figure 1 and found that indeed linear bands are present for one and three layers of graphene, but not for two and four. In particular, the linear bands in the three-layer system show a slope very close to that of graphene.

3.2. Electronic structure from a tight-binding model

Considering the system(s) from a nearest neighbor Hamiltonian perspective [15, 29, 30], we write

$$\mathcal{H} = -t \sum_{\langle m,n\rangle i\sigma} a^{\dagger}_{im\sigma} b_{in\sigma} - t_{\perp} \sum_{ijm\sigma} b^{\dagger}_{im\sigma} b_{jm\sigma} + \text{H.c.}, \qquad (1)$$

where $a^{\dagger}_{im\sigma}$ ($b^{\dagger}_{im\sigma}$) denotes an operator for an electron at site m ($\mathbf{r}_m$) with spin σ in the A(B) sublattice in the ith layer. The parameters for the in-plane hopping and the hopping between the planes are denoted by t (∼3 eV) and $t_{\perp}$ (∼t/10),

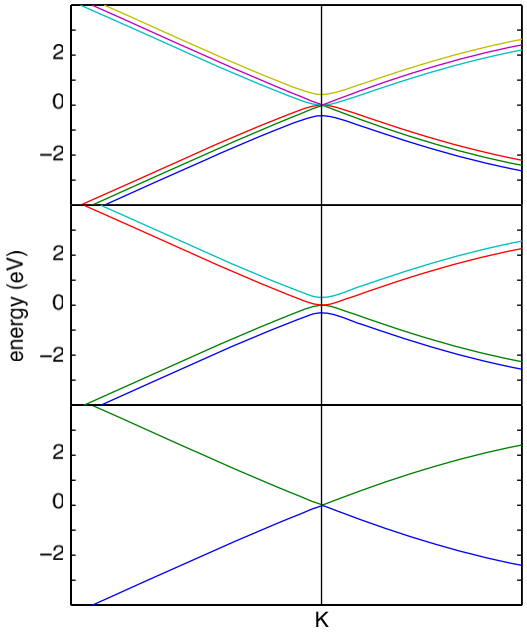

Figure 3. Band structure of the one, two, and three layers of graphene stacked on top of each other, as calculated from the nearest neighbor Hamiltonian in equation (1). Here, $t = 3$ eV and $t_\perp = t/10$.

respectively. Transforming the site operators to **k**-space, using

$$a_{im\sigma} = \frac{1}{\sqrt{N}} \sum_{\mathbf{k}} a_{i\mathbf{k}\sigma} \mathrm{e}^{-\mathrm{i}\mathbf{k}\cdot\mathbf{r}_m},$$
$$b_{im\sigma} = \frac{1}{\sqrt{N}} \sum_{\mathbf{k}} b_{i\mathbf{k}\sigma} \mathrm{e}^{-\mathrm{i}\mathbf{k}\cdot\mathbf{r}_m}, \tag{2}$$

we obtain a **k**-space model, by means of which we numerically calculate the band structure near the K (K′) points in the Brillouin zone, see figure 3. Our results are in agreement with previous nearest neighbor model calculations for one-layer (lower panel) and two-layer (middle panel) graphene [29, 30], as well as for three-layer graphene (upper panel) [24]. More importantly though, is that the basic features of the band structures calculated within FP-LMTO method are captured by means of the nearest neighbor description, thus showing that other interaction parameters, e.g. next nearest neighbor interactions etc, are redundant for the basic qualitative picture.

3.3. Dielectric response

The imaginary part of the optical dielectric function is calculated as (see e.g. [22])

$$\epsilon_2^{ij}(\omega) \propto \frac{1}{V} \sum_{\mathbf{k}nn'} \langle \mathbf{k}n|p_i|\mathbf{k}n'\rangle \langle \mathbf{k}n'|p_j|\mathbf{k}n\rangle \times f_{\mathbf{k}n}(1 - f_{\mathbf{k}n'}) \times \delta(e_{\mathbf{k}n'} - e_{\mathbf{k}n} - \hbar\omega) \tag{3}$$

where $\langle \mathbf{k}n|p_i|\mathbf{k}n'\rangle$ is the expectation value of the momentum operator between band states $|n\rangle$ and $|n'\rangle$ for states with the crystal momentum **k**, i (and j) $= x$, y, or z, and V is the volume of the unit cell of the crystal. In a calculation of graphene, which is a two-dimensional object, one has to make a somewhat arbitrary choice of the volume of the C atoms of the two-dimensional unit cell. We have chosen to use a volume of these C atoms which is the same as the volume of C in graphite. In practice then, the calculations were made for a cell with extended c-axis, in order to simulate isolated C layers, and the numerical value of $\epsilon_2^{ij}(\omega)$ was scaled to correspond to a volume V which is that of graphite.

Our computed dielectric functions (real and imaginary parts, albeit without a Drude component) for graphite and for one, two, and three graphene layers are presented respectively in figure 4. Results for the x-component of the momentum operator (see equation (3)) (ϵ_{xx}) are presented in full (black) lines, while the results corresponding to the z-component of the momentum operator (ϵ_{zz}) are in dashed (red) lines. The data in figure 4 agree rather well with published data for graphite [22]. In [22] a comparison between experimental and theoretical data for graphite was made, and it was observed that the agreement was satisfactory. Also, our results agree well with those of Marinopoulos [31]. For graphite [22], the observed features are mostly due to transitions between π and π^* states (for the 4 eV peak), and to transitions between σ and σ^* states on the high-symmetry line between Γ and M.

The data in figure 4 suggest that, concerning the real and imaginary parts of ϵ, the calculated values are quite independent of the number of graphene layers, i.e. the curves in figure 4 are essentially independent of the number of C layers. The main effect of the thickness can be found for ϵ_{zz}, where for one single layer of graphene, the transition between π and π^* states is forbidden [22], so ϵ_{zz} is exactly zero between 0 and ∼10 eV. For two and three graphene layers, these transitions are not strictly forbidden but they remain very weak.

3.4. Elastic constants

The theory of elasticity of three-dimensional objects can be cast in a simple equation

$$E(V, \delta) \approx E(V_0, 0) + V_0 \sum_i \tau_i \varsigma_i \delta_i + \frac{V_0}{2} \sum_{ij} C_{ij} \varsigma_i \delta_i \varsigma_j \delta_j, \tag{4}$$

where $E(V_0, 0)$ is the total energy of the undistorted system at volume V_0, the sums run over Voigt index 1–6, ς_i takes the value 1 if the Voigt index is 1, 2, or 3, and it takes the value 2 if the Voigt index takes the values 4, 5, or 6. Furthermore, τ_i is an element of the stress tensor and C_{ij} is the elastic constant [32]. δ refers to the strain. For a two-dimensional object like graphene the theory of elasticity becomes somewhat modified, as discussed, for example, by Behroozi [33]. Hence, the expression in equation (4) is modified to

$$E(A, \delta) \approx E(A_0, 0) + A_0 \sum_i \tau_i \delta_i + \frac{A_0}{2} \sum_{ij} C_{ij} \varsigma_i \delta_i \varsigma_j \delta_j, \tag{5}$$

where A_0 is the area of the unit cell. For a three-dimensional hexagonal lattice there are five elastic constants C_{11}, C_{12}, C_{13}, C_{33}, and C_{55}, which for the two-dimensional hexagonal lattice of graphene reduces to only C_{11} and C_{12}. Because the expression in equation (5) involves an area instead of a volume in front of the summation, the unit of the two-dimensional

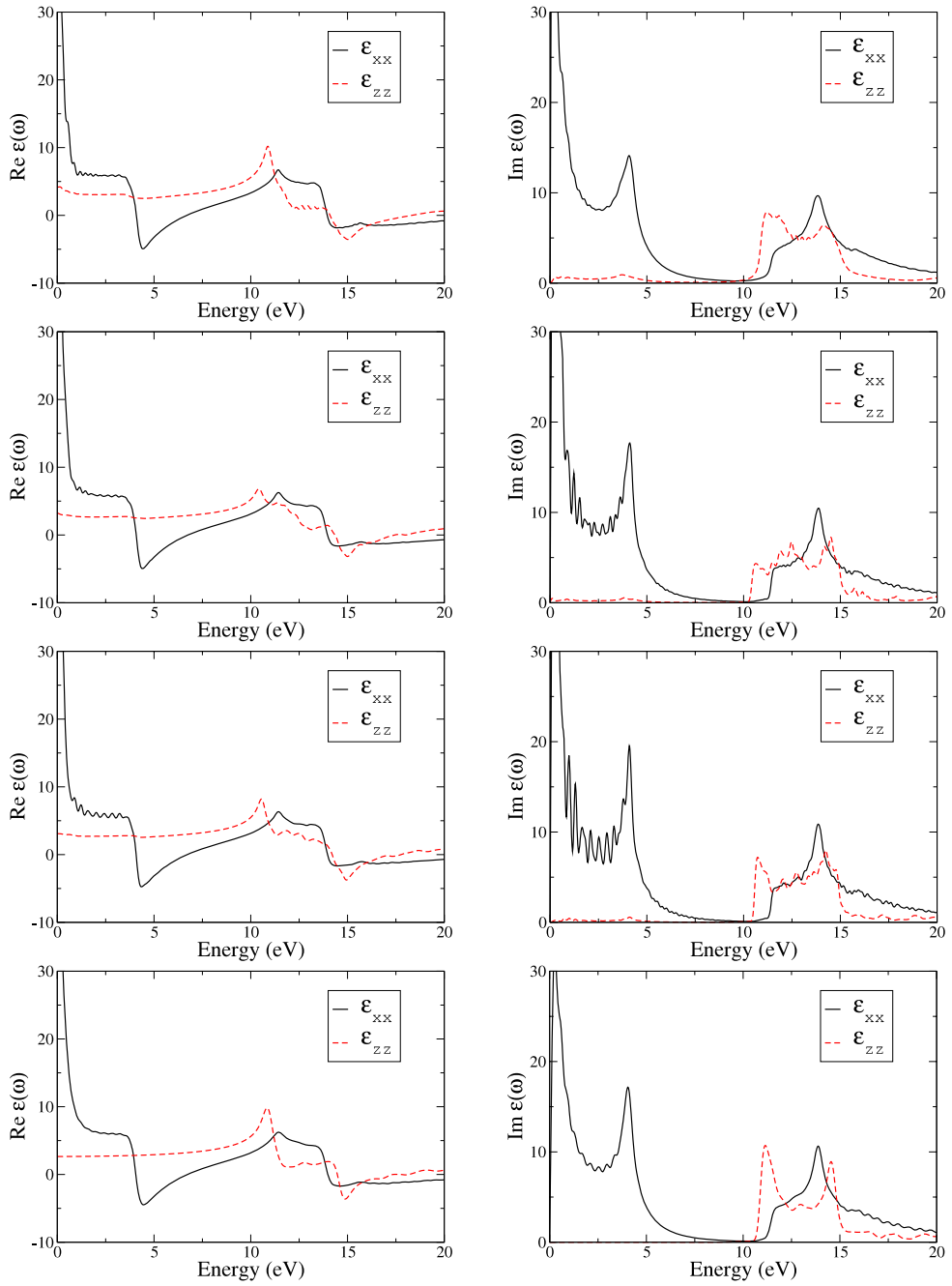

Figure 4. Real (left column) and imaginary (right column) part of the dielectric function of graphite (upper panel), and of three (second upper panel), two (second lower panel), and one (lower panel) layers of graphene.

elastic constant is different than that of a three-dimensional elastic constant, where the unit is Pa. Hence the unit of the two-dimensional elastic constant is m Pa. We will below report on our calculated elastic constants of graphene in this unit.

In figures 5 and 6 we show the calculated total energy versus distortions corresponding to the elastic constants c_{11} and c_{12}, respectively. It should be noted that we display the energy per C atom. As is obvious from the two figures, the different systems react very similarly to distortion with roughly the same energy cost. Hence, the expansion coefficients for bulk graphite as well as for graphene, two-layer graphene and three-layer graphene are all very similar. This is consistent with the fact that the chemical binding which is relevant for these two distortions is governed by the sp^2 bonds, which are very similar for the four systems shown in figures 5 and 6.

For graphite the calculated distortions correspond to a value of $c_{11} = 1.098$ Mbar and $c_{12} = 0.154$ Mbar. Both values reproduce with acceptable accuracy the experimental values, see table 1. This gives credit to the accuracy of the calculations and enables us to trust the elastic constants of graphene, two-layer graphene and three-layer graphene. The elastic constants for these systems are also listed in table 1. Unfortunately we are not aware of any experimental data with which to compare these numbers, and hence our theory serves as a

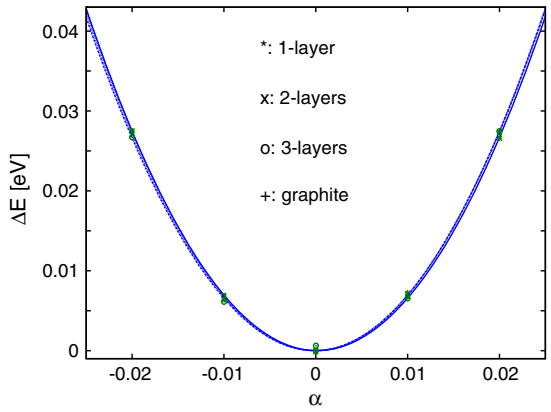

Figure 5. The calculated total energy as a function of distortion. $C_{11} + C_{12}$ is calculated using $\alpha_{xx} = \alpha$, $\alpha_{yy} = \alpha$, and with the other elements of the distortion matrix $\alpha_{ij} = 0$.

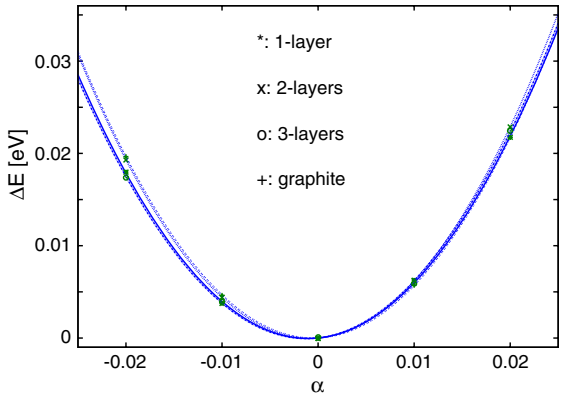

Figure 6. The calculated total energy as a function of distortion. $C_{11} - C_{12}$ is calculated using $\alpha_{xx} = \alpha$, $\alpha_{yy} = -\alpha$ and with the other elements of the distortion matrix $\alpha_{ij} = 0$.

prediction. We note, however, that experimental studies of the elasticity of graphene have been published recently, reporting on the Young's modulus [34]. Michel and Verberck [35] have calculated the elastic constants for graphite and tension coefficients ($c_{ij} \approx 2\gamma_{ij}/c$) for graphene using the Born long wave method to obtain phonon dispersion. Table 1 shows that the elastic constants for graphite reported in [35] are too large compared to experiment (10% and 70% for c_{11} and c_{12}, respectively). Because we consistently report smaller elastic constant and tension coefficients compared to [35] we are confident of the accuracy of the first-principles calculations in this paper.

4. Conclusion

In this paper we have studied theoretically several material properties when going from one C layer in graphene to two and three graphene layers and on to graphite. The properties we have focused on are the elastic constants, electronic structure (energy bands and densities of states), and the dielectric properties. In general we find very similar behavior for all studied systems. For any of the properties we have looked at, the modification due to an increase in the number of graphene layers is within a few per cent. The largest effect due to the thickness is found for ϵ_{zz} which is zero in the energy interval of 0–∼10 eV for monolayer graphene, and non-zero for thicker layers, including graphite. The similarity in elastic constants, C_{11} and C_{12}, for the systems studied here is naturally due to these constants being determined by the covalent in-plane sp^2 hybrids, which are essentially the same and independent of thickness. Our results are in agreement with the analysis presented recently by Kopelevich and Esquinazi [42].

Table 1. Elastic constants of graphite (in TPa) and of graphene (in Pa m) for one, two, and three C layers. The tension coefficients (γ_{11}, γ_{12}, and γ_{66}) for graphene are given in 10^4 dyn cm^{-1}. Note that c_{66} is given through the relation $c_{66} = (c_{11} - c_{12})/2$. In experiment, c_{11} and c_{66} are measured and c_{12} is computed via the previous expression. Numbers in square brackets have been calculated based on the numbers on the same row, i.e. not explicitly shown in the corresponding reference.

Material	$c_{11} + c_{12}$	c_{11} (γ_{11})	c_{12} (γ_{12})	c_{66} (γ_{66})
Graphite present	1.252	1.098	0.154	0.472
Calc. [35]	[1.487]	1.211	0.276	0.468
Calc. [36]	1.283			
Exp. [37]	1.240			
Exp. [38–40]	[1.240]	1.060	0.180	0.442
Exp. [41]	[1.248]	1.109	0.139	0.485
Exp. [40]	[1.24]	1.06	[0.18]	0.44
One-layer present		358 (35.8)	55.0 (5.50)	152 (15.2)
One-layer calc. [35]		(40.6)	(9.2)	(15.7)
Two-layers present		368 (36.8)	47.3 (4.73)	160 (16.0)
Three-layers present		358 (35.8)	54.5 (5.45)	152 (15.2)

Acknowledgments

We acknowledge support from the Swedish Research Council (VR), Swedish Foundation for Strategic Research (SSF), the Swedish National Allocations Committee (SNIC/SNAC), and the Göran Gustafsson Stiftelse. SL acknowledges financial support from ANR PNANO Grant ANR-06-NANO-053-02 and ANR Grant ANR-BLAN07-1-186138.

References

[1] Geim A K and Novoselov K S 2007 *Nat. Mater.* **6** 183
[2] Meyer J C, Geim A K, Katsnelson M I, Novoselov K S, Booth T J and Roth S 2007 *Nature* **446** 60
[3] Novoselov K S, Geim A K, Morozov S V, Jiang D, Katsnelson M I, Grigorieva I V, Dubonos S V and Firsov A A 2005 *Nature* **438** 197
[4] Katsnelson M I, Novoselov K S and Geim A K 2006 *Nat. Phys.* **2** 620
[5] Novoselov K S, McCann E, Morozov S V, Falko V I, Katsnelson M I, Zeitler U, Jiang D, Schein F and Geim A K 2006 *Nat. Phys.* **2** 177
[6] Novoselov K S, Geim A K, Morozov S V, Jiang D, Zhang Y, Dubonos S V, Grigorieva I V and Firsov A A 2004 *Science* **306** 666
[7] Novoselov K S, Jiang Z, Zhang Y, Morozov S V, Stormer H L, Zeitler U, Maan J C, Boebinger G S, Kim P and Geim A K 2007 *Science* **315** 1379
[8] Pendry J B 2007 *Science* **345** 1226
Cheianov V V, Falko V and Altshuler B L 2007 *Science* **315** 1252

[9] Wills J M, Eriksson O, Alouani M and Price D L 2000 *Electronic Structure and Physical Properties of Solids: the Uses of the LMTO Method* (Berlin: Springer)
[10] Kresse G and Furthmüller J 1996 *Comput. Mater. Sci.* **6** 15
[11] Kresse G and Joubert D 1999 *Phys. Rev.* B **59** 1758
[12] Blöchl P E 1994 *Phys. Rev.* B **50** 17953
[13] Perdew J P, Burke K and Ernzerhof M 1996 *Phys. Rev. Lett.* **77** 3865
[14] Monkhorst H J and Pack J D 1976 *Phys. Rev.* B **13** 5188
[15] Wallace P R 1947 *Phys. Rev.* **71** 622
[16] McClure J W 1957 *Phys. Rev.* **108** 612
[17] Ferrari A C *et al* 2006 *Phys. Rev. Lett.* **97** 187401
[18] Graf D *et al* 2007 *Nano Lett.* **7** 238
[19] Reich S, Maultzsch J, Thomsen C and Ordejon P 2002 *Phys. Rev.* B **66** 035412
[20] Henrard L and Latil S 2006 *Phys. Rev. Lett.* **97** 036803
[21] Trevisanutto P E *et al* 2008 *Phys. Rev. Lett.* **101** 226405
[22] Ahuja R, Auluck S, Wills J M, Alouani M, Johansson B and Eriksson O 1997 *Phys. Rev.* B **55** 4999
[23] Boettger J C 1997 *Phys. Rev.* **55** 11202
[24] Partoens B and Peeters F M 2006 *Phys. Rev.* B **74** 075404
[25] Luk'yanchuk I A and Kopelevich Y 2004 *Phys. Rev. Lett.* **93** 166402
[26] Luk'yanchuk I A and Kopelevich Y 2006 *Phys. Rev. Lett.* **97** 256801
[27] Lebègue S and Eriksson O 2009 *Phys. Rev.* B **79** 155409
[28] Partoens B and Peeters F M 2007 *Phys. Rev.* B **75** 193402
[29] Peres N M R, Guinea F and Castro Neto A H 2006 *Phys. Rev.* B **73** 125411
[30] Nilsson J, Castro Neto A H, Peres N M R and Guinea F 2006 *Phys. Rev.* B **73** 214418
[31] Marinopoulos A G, Reining L, Rubio A and Olevano V 2004 *Phys. Rev.* B **69** 245419
[32] Fast L, Wills J M, Johansson B and Eriksson O 1995 *Phys. Rev.* B **51** 17431
[33] Behroozi F 1996 *Langmuir* **12** 2289
[34] Lee C, Wei X, Kysar J W and Hone J 2008 *Science* **321** 385
[35] Michel K H and Verberck B 2008 *Phys. Status Solidi* b **245** 2177
Michel K H and Verberck B 2008 *Phys. Rev.* B **78** 085424
[36] Mounet N and Marzari N 2005 *Phys. Rev.* B **71** 205214
[37] Delhaes P (ed) 2001 *Graphite and Precursors* (Amsterdam: Gordon and Breach) chapter 6
[38] Blackslee O L, Proctor D G, Seldin E J, Spence G B and Weng T 1970 *J. Appl. Phys.* **41** 3373
[39] Seldin E J and Nezbeda C W 1970 *J. Appl. Phys.* **41** 3389
[40] Nicklow R, Wakabayashi N and Smith H G 1972 *Phys. Rev.* B **5** 4951
[41] Bosak A, Krisch M, Mohr M, Maultzsch J and Thomsen C 2007 *Phys. Rev.* B **75** 153408
[42] Kopelevich Y and Esquinazi P, unpublished